Surface Review and Letters, Vol. 16, No. 1 (2009) 105–110

World Scientific
www.worldscientific.com

ELECTRONIC STRUCTURE AND BAND BENDING OF MODULATION-DOPED GaAs/Al_x Ga_{1-x}As SYMMETRIC AND ASYMMETRIC DOUBLE QUANTUM WELLS UNDER AN APPLIED ELECTRIC FIELD

F. UNGAN*, E. KASAPOGLU*,‡, H. SARI* and I. SÖKMEN†
*Cumhuriyet University, Physics Department, 58140 Sivas, Turkey
†Dokuz Eylül University, Physics Department, 35160 Izmir, Turkey
‡ekasap@cumhuriyet.edu.tr

Received 9 July 2008

In this study, we have calculated theoretically the effects of the electric field and doping concentration on the sub-band energies, the electron population, and total charge density in modulation-doped symmetric and asymmetric GaAs/$Al_{0.33}Ga_{0.67}$As double quantum wells. Electronic properties of the system are determined by the solving the Schrödinger and Poisson equations self-consistently in the effective-mass approximation. The application of an electric field in the growth direction of the system causes a polarization of the carrier distribution and shifts the sub-band energies, which may be used to control and modulate intensity output devices. In an asymmetric double-quantum-well structure, the effects mentioned above appear more clearly.

Keywords: Low-dimensional systems; double quantum well.

1. Introduction

During the last decade, GaAs/AlGaAs double quantum wells have been intensively investigated because of their potential applications in advanced optoelectronic devices. Recently, the evolution of the growth techniques such as molecular beam epitaxy (MBE) and metal-organic chemical vapor deposition (MOCVD) combined with the use of the modulation-doping technique made it possible to achieve a new two-dimensional system at the semiconductor heterojunction interface between GaAs and $Al_xGa_{1-x}As$.[1–4] In this system, the wide gap material (GaAs/Al_x Ga_{1-x}As) is modulation doped, while the narrow gap material (GaAs) is undoped. Since the ionized impurity scattering is greatly reduced by separating the electrons from their parent donors and the Coulomb scattering is reduced by the screening effects due to the extremely high density of the two-dimensional electron gas, high electron mobilities can be obtained in this structure. Under equilibrium conditions, electrons in donor levels of $Al_xGa_{1-x}As$ are transferred to the GaAs layer, leading to considerable band bending. Many electronic and optical devices have been developed based on these structures.

The determination of the sub-band structure and the study of many-body effects are fundamental problems related to those systems, which can be well understood through comparisons between experimental and theoretical calculations. Owing to its importance in revealing the electron-electron many-body interactions such as the exchange–correlation

‡Corresponding author.

effects in low electronic density and the Coulomb drag effects, plasmon modes in double-quantum-well (DQW) structures have attracted a great deal of theoretical[5−14] and experimental[15,19] interested.

Asymmetric double-quantum-well (ADQW) structures, namely, two adjacent wells of different thickness, are the ideal structures for investigating the mechanisms of carrier transfer. In the widely investigated case of ADQWs separated by thin barriers, resonant,[20,21] nonresonant,[22,23] and coherent[24,25] tunnelling have been studied in detail.

We investigated the dependence of symmetric (or asymmetric) modulation-doped DQW on the temperature, exchange-correlation potential, and the same (or different) doping concentration in Refs. 26 and 27. The purpose of present study is to theoretically investigate the sub-band structure of modulation-doped symmetric and asymmetric DQWs as dependent on the doping concentration and electric field. At the end, it has been found that the changes in the potential profile, sub-band energies, and the sub-band populations depend on the doping concentration and electric field.

2. Theory

The electronic structure of modulation-doped DQW under the electric field has been investigated by using a self-consistent calculation in the effective-mass approximation. We have calculated the confinement potential, charge density, sub-band energies, and sub-band populations by solving the Schrödinger and Poisson equations self-consistently.

The structure of the DQW system is given in Fig. 1. The origin of the z-axis is taken at the center of the structure. It consists of two GaAs wells with Lw_1 and Lw_2 widths, separated by an undoped $Al_xGa_{1-x}As$ barrier with L_b width and adjacent to two $Al_xGa_{1-x}As$ barrier layers. Each of these two barrier layers consists of an undoped spacer layer with Ls_1 and Ls_2 widths. The depletion lengths Ld_m and Ld_p are determined self-consistently in our calculations. In the effective-mass approximation, the single electron one-dimensional Schrödinger equation can be written as

$$\left(-\frac{\hbar^2}{2m^*}\frac{d^2}{dz^2}+V(z)\right)\psi_i(z)=E_i\psi_i(z) \qquad (1)$$

and

$$V(z)=V_H(z)+eFz, \qquad (2)$$

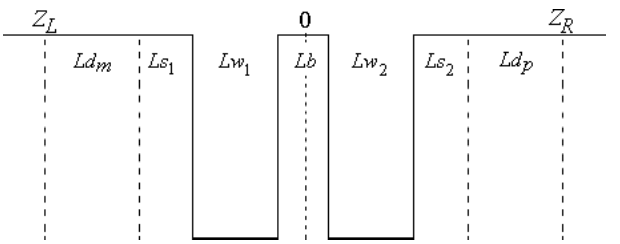

Fig. 1. The schematic representation of DQW structure. Ld_m and Ld_p are doped $Al_{0.33}Ga_{0.67}As$ thicknesses, Ls_1 and Ls_2 are undoped $Al_{0.33}Ga_{0.67}As$ thicknesses, Lw_1 and Lw_2 are GaAs quantum well widths, Lb is the barrier width, and $L_D = Z_L + Z_R$ is the total thickness of DQW structure.

where m^* is the electron effective mass. $V_H(z)$is the effective Hartree potential and F is the strength of the applied electric field. The Hartree potential $V_H(z)$ is obtained by solving the Poisson equation:

$$\frac{d^2V_H(z)}{dz^2}=-\frac{4\pi e^2}{\varepsilon}[N(z)-N_d(z)], \qquad (3)$$

where ε is the GaAs dielectric constant and $N_d(z)$ is the total density of ionized dopants. The electron density is related to the wave functions as

$$N(z)=\sum_{i=1}^{n_d} n_i|\psi_i(z)|^2, \qquad (4)$$

where n_d is the number of filled states, n_i is the temperature-dependent number of electrons per unit area in the ith sub-band given by

$$n_i=\frac{m^*k_BT}{\pi\,\hbar^2}\ \ln\{1+\exp[(E_F-E_i)/k_BT]\}, \qquad (5a)$$

and at zero temperature

$$n_i=\frac{m^*}{\pi\,\hbar^2}(E_F-E_i), \qquad (5b)$$

where i is sub-band index, k_B is Boltzmann constant, and E_F is Fermi energy. According to Ref. 16, at the low-temperature limit ($T\to 0$), the Fermi energy can be taken as the donor level, which is supposed to lie at an energy $E_F = 0.070\,\text{eV}$ below the conduction band of the GaAs layers. All donors are assumed to be ionized, i.e.

$$Ld_m\times Nd_1+Ld_p\times Nd_2=\sum_{i=1}^{n_d} n_i, \qquad (6)$$

where Nd_1 is the doping concentration for Ld_m thickness and Nd_2 is the doping concentration for Ld_p thickness. The potential profile, density

profile, sub-band energies, and sub-band populations are obtained from self-consistently solution of Eqs. (1)–(6).

3. Results and Discussion

In this study, we have investigated theoretically the electronic structure of modulation-doped $GaAs/Al_{0.33}Ga_{0.67}As$ DQW under an electric field applied along the growth direction for different doping concentrations. We have studied two different DQW structures. The dimensions of the structures are $Lw_1 = Lw_2 = 100\,\text{Å}$ with $L_b = 75\,\text{Å}$ for the symmetric case, whereas $Lw_1 = 100\,\text{Å}$ and $Lw_2 = 75\,\text{Å}$ asymmetric one. Furthermore, the barrier layers have same thickness ($Ls_1 = Ls_2 = 10\,\text{Å}$ and $Ld_m = Ld_p$) and the same doping concentration ($Nd_1 = Nd_2$).

In Figs. 2 (a) and 2(b), the confinement potentials, the sub-band energies, and the squared wave functions belonging to these energy levels for a fixed doping concentration ($Nd_1 = 5 \times 10^{17}\,\text{cm}^{-3}$) and $E_F = 70\,\text{meV}$ at $T = 0\,\text{K}$ are given for symmetric and asymmetric DQWs, respectively. Solid (dashed) curves are corresponding to $F = 0$ ($F = 10\,\text{kV/cm}$).

As shown Fig. 2(a), the sub-band energy levels appear as doublets because of tunnelling between the two wells.[26] When the electric field is applied, degeneracy is broken and the sub-band energy levels are separated from each other. Electron shifts to the left side of the structure with the effect of the electric field.

As shown in Fig. 2(b), the left well is wider than the right one. The asymmetry breaks the degeneracy of the two confined states and this results in the lower energy state (E_1) being more localized in the wider left-hand well and the higher energy state (E_2) being associated with the narrower right-hand one. When the electric field is applied, the depth of the potential in the left well increases while the depth of the potential corresponding to the right well decreases and so, the energy levels are separated from each other.

The effects on potential profile of electric field, for two different doping concentrations, are shown in Figs. 3(a) and 3(b), respectively. In self-consistent calculation, we assume that Fermi energy is constant at $T = 0\,\text{K}$ (i.e. $E_F = Ed$). In this figure, the Fermi energy is set to 0 eV. As seen in these figures, as doping concentration increases, the band bending increases. It has been shown that when we apply electric field to the structure, in addition to effects that doping concentration has made, the well on the left gets more deeper and finally, band bending increases with the electric field and doping concentration.

In Figs. 4(a) and 4(b), the variation of the sub-band energy levels as a function of doping concentration for $F = 0$ (solid lines) and $F = 10\,\text{kV/cm}$ (dashed lines) electric field values are given for symmetric and asymmetric DQWs, respectively. With increasing doping concentration and applied electric field, the depth of the potential profile, the sub-band energies and populations, and the density profiles are importantly changed. At high doping concentration, an increasing charge density in the doped layer leads to more band bending and gives rise to the formation of a deeper quantum well. Since the applied electric field would increase the density of the electrons in the left well and also decrease the density of electrons in the right well, the energy levels are separated from each other in symmetric double quantum well, while the energy levels are brought closer together in asymmetric double quantum well.

The change in the sub-band populations is investigated depending on the change in doping concentration and applied electric field. The relationship between these variables is shown in Figs. 5(a) and 5(b). As expected from the finding in Figs. 4(a) and 4(b), as the electric field and doping concentration increase, the sub-band population in the left well increases, while the sub-band population in the right well decreases.

For different doping concentrations ($N_d = 1 \times 10^{17}\,\text{cm}^{-3}$ and $N_d = 5 \times 10^{17}\,\text{cm}^{-3}$), the changes in the carrier density profile – $N(z)$ of the system with the doping concentration and applied electric field are displayed in Figs. 6(a) and 6(b). As seen in these figures, with the decrease in the doping concentration, while the electron density in Lw_1 increases, the electron density in Lw_2 decreases. In the coupled DQW structure, the electron wave functions can easily penetrate into the barriers, and this results in more carriers distributing the left well. Since, at high doping concentration, the potential corresponding to the Lw_1 region is deeper than in Lw_2, the electrons in the Lw_2 region move to the Lw_1 region, and so, the carrier density in the left well increases.

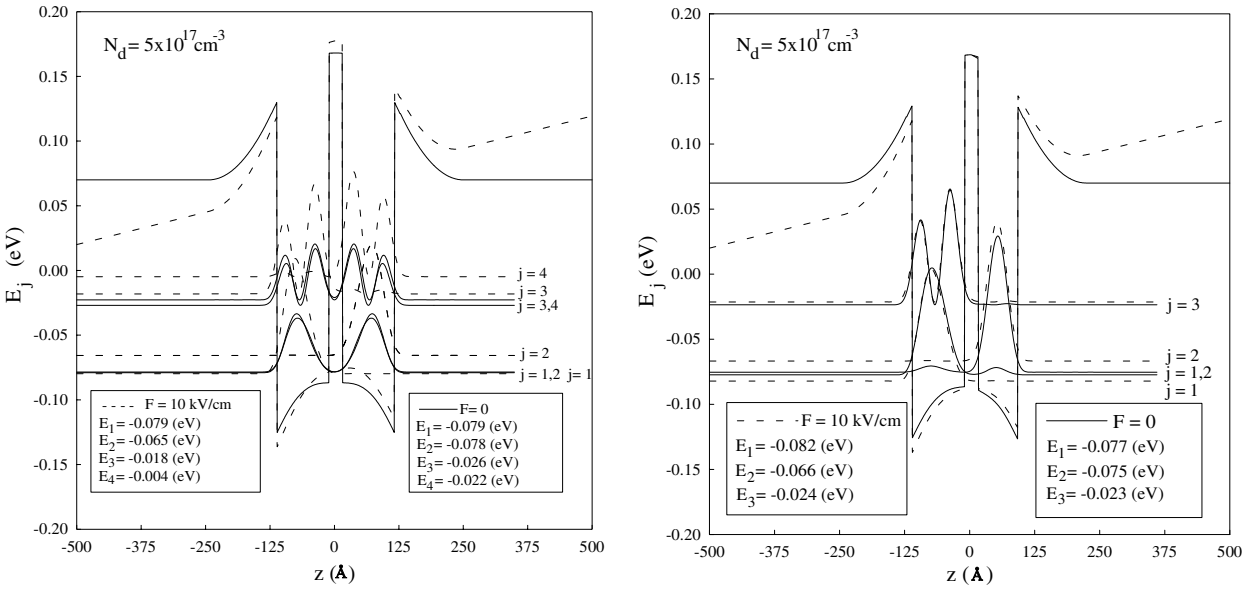

(a) (b)

Fig. 2. For doping concentration $N_d = 5 \times 10^{17}\,\mathrm{cm}^{-3}$, the confinement potential profile, first four sub-band energy levels, and the squared wave functions belonging to these energy levels in (a) symmetric and (b) asymmetric DQW, respectively. Solid (dashed) curves are corresponding to $F = 0$ ($F = 10\,\mathrm{kV/cm}$).

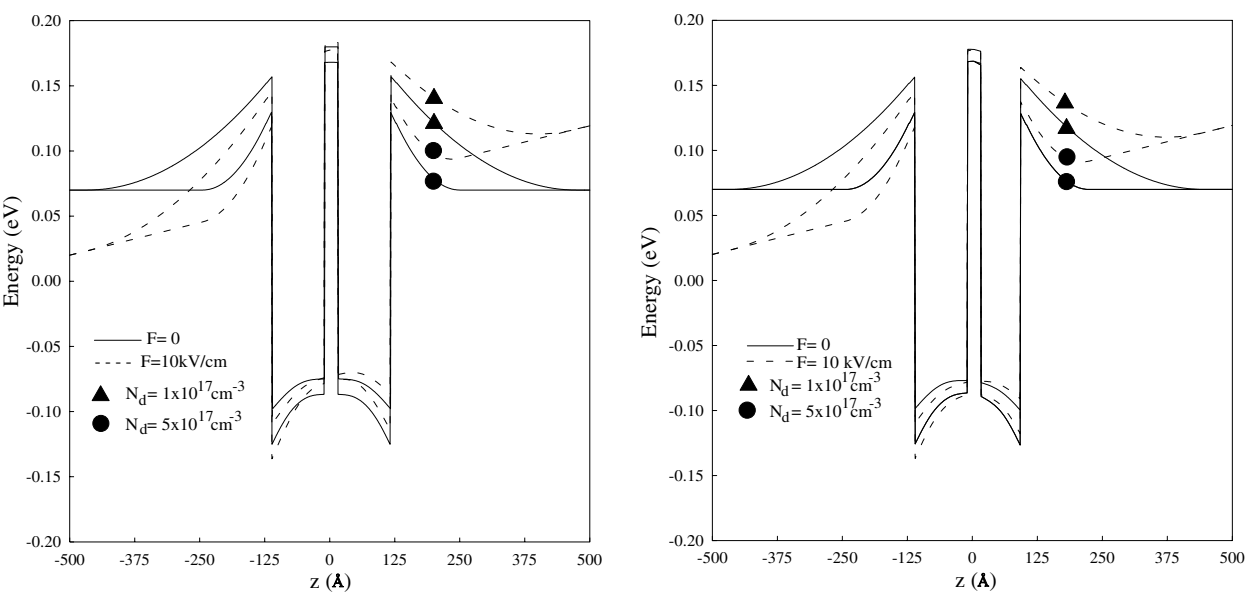

(a) (b)

Fig. 3. The variation of the confinement potential according to the electric field and doping concentration in (a) symmetric and (b) asymmetric DQW. Fermi energy is set to 0 eV. Solid (dashed) curves are corresponding to $F = 0$ ($F = 10\,\mathrm{kV/cm}$).

In conclusion, we have investigated the electronic structure of $GaAs/Al_{0.33}Ga_{0.67}As$ symmetric and asymmetric DQW under an applied electric field. To determine the sub-band structure, the self-consistent methods of the Schrödinger and Poisson equations have been used. We have studied the effect of the electric field together with the doping concentration. As a result, we have seen that the

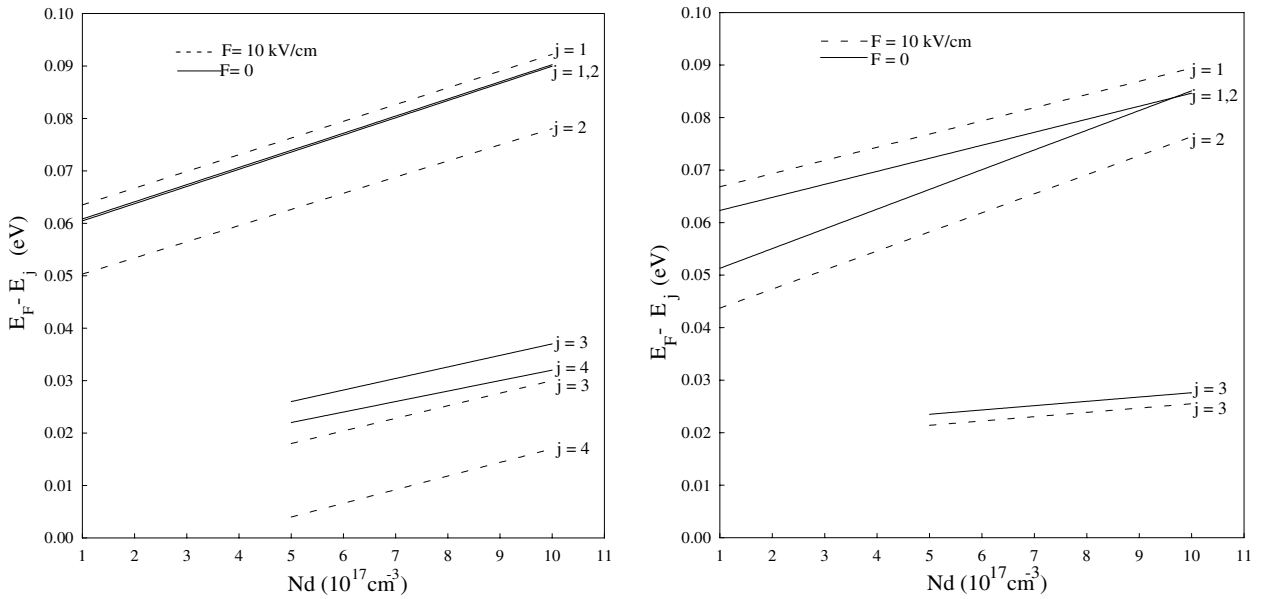

Fig. 4. The variation of the sub-band energy levels as a function of doping concentration for $F = 0$ (solid lines) and $F = 10\,\mathrm{kV/cm}$ (dashed lines) electric field values in (a) symmetric and (b) asymmetric DQW.

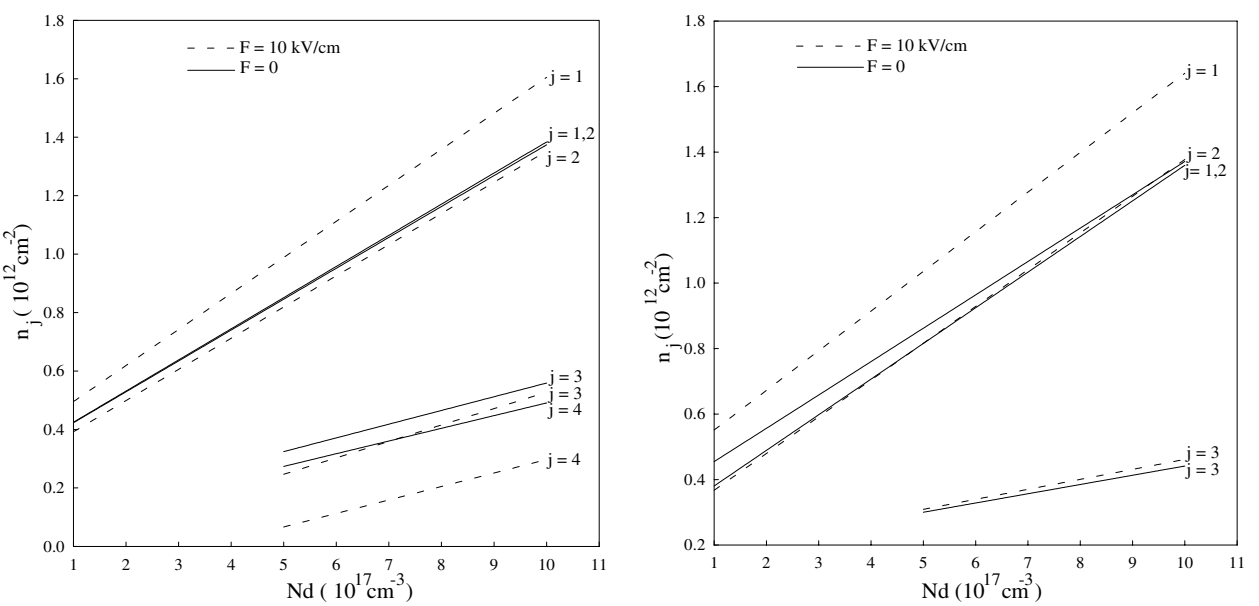

(a) (b)

Fig. 5. The variation of the electron populations vs the doping concentration for $F = 0$(solid lines) and $F = 10\,\mathrm{kV/cm}$(dashed lines) electric field values in (a) symmetric and (b) asymmetric DQW, respectively.

high doping concentration and applied electric field lead to significant changes of electronic structure of modulation-doped DQW; thus, the donor concentration and electric field can be used as a tuning parameter for semiconductor devices. More examples of the modulation-doped potentials with an externally applied electric field and their applications to electronic devices based on the inter-sub-band transitions and resonant tunnelling diodes can be designed by considering these results.

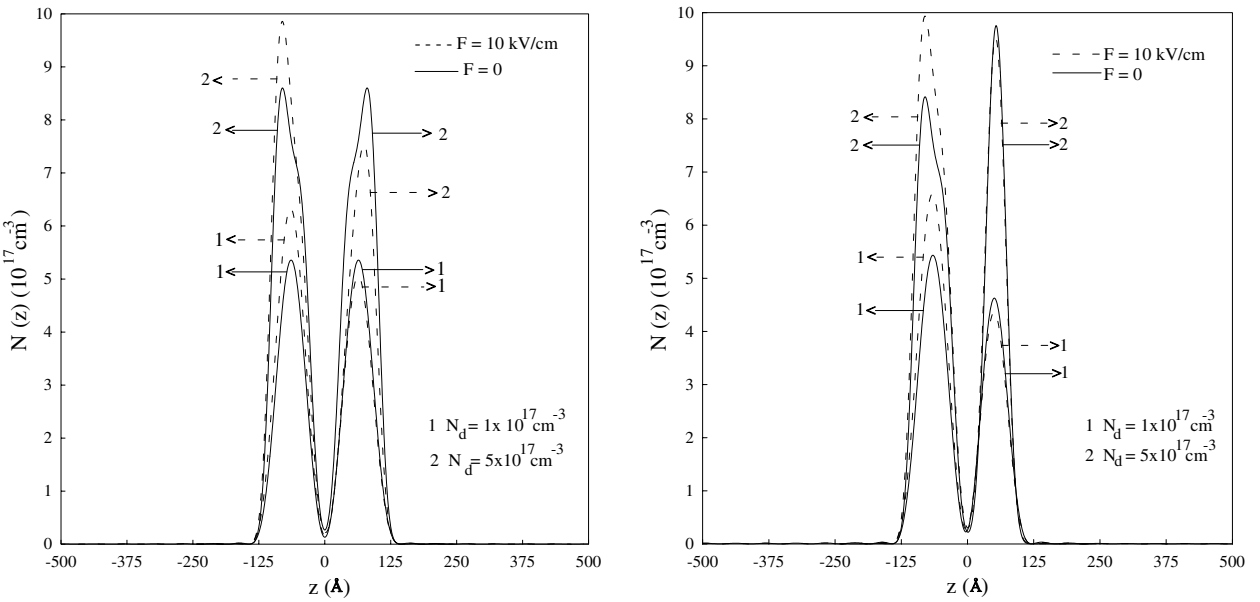

Fig. 6. The total charge density for different doping concentrations in (a) symmetric and (b) asymmetric DQW for $F = 0$ (solid lines) and $F = 10$kV/cm (dashed lines).

References

1. R. Dingle, H. L. Störmer, A. C. Gossard and W. Weigmann, *Appl. Phys. Lett.* **33** (1978) 665.
2. L. Esaki and R. Tsu, *IBM Res. Rep.* **RC-2418** (1969).
3. H. L. Störmer, R. Dingle, A. C. Gossard, W. Weigmann and M. D. Sturge, *J. Vacl. Sci. Techno.* **16** (1979) 1517.
4. E. E. Mendez and K. von Klitzing, *Physics and Applications of Quantum Wells and Superlatices* (Plenum Press, New York, London, 1987).
5. S. Das Sarma and A. Madhukar, *Phys. Rev. B* **23** (1981) 805.
6. G. E. Santoro and G. F. Giuliani, *Phys. Rev. B* **37** (1988) 937.
7. J. K. Jain and S. Das Sarma, *Phys. Rev. B* **36** (1987) 5949.
8. S. Das Sarma and P. I. Tomborenea, *Phys. Rev. Lett.* **73** (1994) 1971.
9. L. Liu, L. Swierkowski, D. Neilson and J. Szymaiski, *Phys. Rev. B* **53** (1996) 7923.
10. P. G. Bolcatto and C. R. Proetto, *Phys. Stat. Sol. B* **220** (2000) 65.
11. G. Gumbs and G. B. Aizin, *Phys. Rev. B* **51** (1995) 7074.
12. S. Das Sarma and E. H. Hwang, *Phys. Rev. Lett.* **81** (1998) 4216.
13. L. Wendler and T. Kraft, *Phys. Rev. B* **54** (1996) 11436.
14. S.-J. Cheng and R. R. Gerhardts, *Phys. Rev. B* **63** (2001) 35314.
15. A. S. Plaut, A. Pinczuk, B. S. Dennis, J. P. Eisenstein, L. N. Pfeiffer and K. W. West, *Surf. Sci.* **361/362** (1996) 158.
16. L. Hedin and B. I. Lundqvist, *J. Phys. C* **4** (1971) 2064.
17. N. P. R. Hill, J. T. Nicholls, E. H. Linfield, M. Pepper, D. A. Ritchie, G. A. C. Jones, B. Yu-Kuang Hu and K. Flensberg, *Phys. Rev. Lett.* **78** (1997) 2204.
18. D. S. Kainth, D. Richards, H. P. Hughes, M. Y. Simmons and D. A. Ritchie, *Phys. Rev. B* **57** (1998) R2065.
19. D. S. Kainth, D. Richards, A. S. Bhatti, H. P. Hughes, M. Y. Simmons, E. H. Linfield and D. A. Ritche, *Phys. Rev. B* **59** (1999) 2059.
20. D. Y. Oberli, J. Shah, T. C. Damen, C. W. Tu, T. Y. Chang, D. A. B. Miller, J. E. Henry, R. F. Kopf, N. Sauer and A. E. di Giovanni, *Phys. Rev. B* **40** (1989) 3028.
21. Ph. Roussignol, M. Gurioli, L. Carraresi, M. Colocci, A. Vinattieri, C. Deparis, J. Massies and G. Neu, *Superlatt. Microstruct.* **9** (1991) 151.
22. A. P. Heberle, W. W. Rühle and K. Köhler, *Phys. Stat. Sol. B* **173** (1992) 381.
23. Ph. Roussignol, A. Vinattieri, L. Carraresi, M. Colocci and A. Fasolino, *Phys. Rev. B* **44** (1991) 8873.
24. K. Leo, J. Shah, E. O. Göbel, T. C. Damen, S. Schmitt-Rink, W. Schafer and K. Köhler, *Phys. Rev. Lett.* **66** (1991) 201.
25. H. G. Roskos, M. C. Nuss, J. Shah, K. Leo, D. A. B. Miller, A. M. Fox, S. Schmitt-Rink and K. Köhler, *Phys. Rev. Lett.* **68** (1992) 2216.
26. F. Ungan, E. Ozturk, Y. Ergun and I. Sokmen, *Eur. P-. J. Appl. Phys.* **29** (2005) 1.
27. F. Ungan, E. Ozturk, Y. Ergun and I. Sokmen, *Superlatt. Microstruct.* **41** (2007) 22.